Environmental Research 212 (2022) 113557

Contents lists available at ScienceDirect

Environmental Research

journal homepage: www.elsevier.com/locate/envres

Sources and processes of organic aerosol in non-refractory PM_1 and $PM_{2.5}$ during foggy and haze episodes in an urban environment of the Yangtze River Delta, China

Shuaiyi Li [a,b], Cheng Chen [c], Guang-li Yang [d,c], Jie Fang [a], Yele Sun [e], Lili Tang [c], Hongli Wang [b], Wentao Xiang [f], Hongliang Zhang [g,h], Philip L. Croteau [i], John T. Jayne [i], Hong Liao [a], Xinlei Ge [a], Olivier Favez [j], Yunjiang Zhang [a,b,*]

[a] Jiangsu Key Laboratory of Atmospheric Environment Monitoring and Pollution Control, Collaborative Innovation Center of Atmospheric Environment and Equipment Technology, School of Environmental Science and Engineering, Nanjing University of Information Science and Technology, Nanjing, China
[b] State Environmental Protection Key Laboratory of Formation and Prevention of Urban Air Pollution Complex, Shanghai Academy of Environment Sciences, Shanghai, China
[c] Jiangsu Environmental Monitoring Center, Nanjing, China
[d] Huaian Environmental Monitoring Center of Jiangsu Province, Huaian, China
[e] State Key Laboratory of Atmospheric Boundary Layer Physics and Atmospheric Chemistry, Institute of Atmospheric Physics, Chinese Academy of Sciences, Beijing, China
[f] Key Laboratory of Clinical and Medical Engineering, School of Biomedical Engineering and Informatics, Nanjing Medical University, Nanjing, China
[g] Nanjing Xindahanda Environmental Science and Technology Limited, Nanjing, China
[h] Handix LLC, Boulder, CO, USA
[i] Aerodyne Research, Inc., Billerica, MA, USA
[j] Institut National de l'Environnement Industriel et des Risques, Verneuil-en-Halatte, France

ARTICLE INFO

Keywords:
$PM_{2.5}$ ACSM
Organic aerosol
Sources
Aqueous process
Aerosol light scattering

ABSTRACT

Organic aerosol (OA) generally accounts for a large fraction of fine particulate matter ($PM_{2.5}$) in the urban atmosphere. Despite significant advances in the understanding their emission sources, transformation processes and optical properties in the submicron aerosol fraction (PM_1), larger size fractions - e.g., $PM_{2.5}$ - still deserve complementary investigations. In this study, we conducted a comprehensive analysis on sources, formation process and optical properties of OA in PM_1 and $PM_{2.5}$ under haze and foggy environments in the Yangtze River Delta (eastern China), using two aerosol chemical speciation monitors, as well as a photoacoustic extinctiometer at 870 nm. Positive matrix factorization analysis - using multilinear engine (ME2) algorithm - was conducted on PM_1 and $PM_{2.5}$ organic mass spectra. Four OA factors were identified, including three primary OA (POA) factors, i.e., hydrocarbon-like OA (HOA), cooking OA (COA), and biomass burning OA (BBOA), and a secondary OA (SOA) factor, i.e., oxidized oxygenated OA (OOA). An enhanced $PM_{1\text{-}2.5}$ COA concentration was clearly observed during cooking peak hours, suggesting important contribution of fresh cooking emissions on large-sized particles (i.e., $PM_{1\text{-}2.5}$). The oxidation state and concentration of $PM_{2.5}$ HOA were higher than that in PM_1, suggesting that large-sized HOA particles might be linked to oxidized POA. High contribution (44%) of large-sized OOA to non-refractory $PM_{2.5}$ mass was observed during haze episodes. During foggy episodes, PM_1 and $PM_{2.5}$ OOA concentrations increased as a positive relationship over time, along with an exponential increase in the $PM_{2.5}$-OOA to PM_1-OOA ratio. Meanwhile, OOA loadings increased with the aerosol liquid water content (ALWC) during foggy episodes. Random forest cross-validation analysis also supported the important influence of ALWC on OOA variations, supporting substantial impact of aqueous process on SOA formation during haze and/or foggy episodes. Obtained results also indicated high OOA contributions (21%–36%) and low POA contributions (6%–14%) to the $PM_{2.5}$ scattering coefficient during haze and foggy episodes, respectively. Finally, we could illustrate that atmospheric vertical diffusion and horizontal transport have important but different effects on the concentrations of different primary and secondary OA factors in different particle size fractions.

* Corresponding author. Jiangsu Key Laboratory of Atmospheric Environment Monitoring and Pollution Control, Collaborative Innovation Center of Atmospheric Environment and Equipment Technology, School of Environmental Science and Engineering, Nanjing University of Information Science and Technology, Nanjing, China.
E-mail address: yjzhang@nuist.edu.cn (Y. Zhang).

https://doi.org/10.1016/j.envres.2022.113557
Received 30 March 2022; Received in revised form 14 May 2022; Accepted 20 May 2022
Available online 28 May 2022

1. Introduction

Fine particulate matter ($PM_{2.5}$) is a key factor leading to the formation of urban haze pollution (Zhang et al., 2015a). Long-term exposure to $PM_{2.5}$ seriously threatens human health (Zhang et al., 2019a; Zhang and Cao, 2015). It can substantially reduce atmospheric visibility via aerosol light absorption and scattering, which also influences the earth's radiation budget and global and/or regional climate change (IPCC, 2013). With the advocacy and implementation of global energy conservation and emission reduction policies, accurate identification of $PM_{2.5}$ sources plays a very important role in the formulation of clean air action plans (Hu et al., 2015).

The chemical composition and sources of atmospheric $PM_{2.5}$ are very complex, including direct emissions from pollution sources (so-called primary particulate matter) and secondary particulate matter formed by gaseous precursors in the atmosphere through complex chemical and physical processes (Zhang et al., 2015a). There are still a large of uncertainties in predicting various sources and chemical composition of $PM_{2.5}$ based on chemical transport models. In situ observation could be one of the most effective ways to quantitatively understand the chemical composition and sources of $PM_{2.5}$ (Hu et al., 2013; Huang et al., 2012; Sun et al., 2015, 2018; Zhang et al., 2014, 2019b). Classically, $PM_{2.5}$ chemical composition were generally investigated based on offline analysis techniques (Cao et al., 2012; He et al., 2001). However, the biggest disadvantage of this monitoring method relies in its low temporal resolution, which offered a huge challenge to capture complex evolution of aerosol physical and chemical properties of $PM_{2.5}$ in the real atmosphere. Recently, some online measurement technologies have been developed and applied in field observation of $PM_{2.5}$ chemical composition (Li et al., 2017b; Zhang et al., 2020b). In particular, the Aerodyne aerosol chemical speciation monitor (ACSM), one of the most widely used instruments, can determine highly time-resolved inorganic (including sulfate, nitrate, ammonium and chloride) and organic aerosol (OA) of non-refractory aerosol particles (NR-PM) (Ng et al., 2011a).

By using receptor models, e.g., positive matrix factorization (PMF), the ACSM organic spectral data can be further analyzed into different OA source factors (Huang et al., 2019; Li et al., 2018; Sun et al., 2012, 2018; Zhang et al., 2015c; Zhou et al., 2020). Generally, these OA factors included primary OA (POA) and secondary OA (SOA) compounds. Indeed, the POA factor included hydrocarbon organic aerosols (HOA) (Sun et al., 2013; Zhang et al., 2019b), cooking organic aerosol (COA) (Sun et al., 2013; Zhang et al., 2015b), biomass burning organic aerosol (BBOA) (Lin et al., 2018; Zhang et al., 2015c), and coal burning organic aerosol (CCOA) (Hu et al., 2013; Li et al., 2017a; Sun et al., 2013), while the SOA factor could be linked to oxygenate OA (OOA) that could often be split into less oxidized OOA (LO-OOA) and more oxidized (MO-OOA) subfractions (Zhang et al., 2019b; Zhou et al., 2020). The ACSM with standard configuration – i.e., equipped with a submicron aerodynamic lens and standard vaporizer - was limited to measure non-refractory chemical composition only in PM_1, but it cannot provide chemical information for the whole $PM_{2.5}$ fraction. Recent developments, including $PM_{2.5}$ aerodynamics lens (Williams et al., 2013a) and capture vaporizer (Hu et al., 2017; Xu et al., 2016), now allow to measure the non-refractory chemical composition in $PM_{2.5}$ using the ACSM (Joo et al., 2021; Sun et al., 2020; Xu et al., 2020; Zhang et al., 2017). Based on such $PM_{2.5}$ ACSM measurements, differences in chemical composition between PM_1 and $PM_{2.5}$ have already been investigated at a few worldwide locations (Joo et al., 2021; Sun et al., 2020; Zhang et al., 2017). However, understanding of sources of POA and SOA, as well as major formation processes of SOA, in $PM_{2.5}$ is still limited, especially in highly polluted environment such as eastern China.

Since the ACSM can measure bulk OA aerosols, it is often coupled with aerosol optical instruments to build an aerosol chemical-optical monitoring system and then is applied to investigate the optical properties of different aerosol chemical compositions (Wang et al., 2015; Xie et al., 2019; Zhang et al., 2018, 2020a). However, most previous studies focused on the optical properties of PM_1 (Wang et al., 2015), yet missed such knowledge for haze particle in $PM_{2.5}$. For example, Wang et al. (2015) found that POA and OOA significantly contributed to the PM_1 extinction coefficient, accounting for 13% and 14% of the total extinction coefficient during heating seasons in urban Beijing, respectively. In urban Beijing, Xie et al. (2019) further found that fossil-fuel emissions (e.g., coal combustion) could contribute up to 55% of the total absorption by light-absorbing OA (i.e., brown carbon). Wang et al. (2016) found that total OA in PM_1 could contribute to 38% of the PM_1 extinction coefficient during springtime in Nanjing. In the Greater Paris area (France), Zhang et al. (2020a) found that residential wood burning was the main source to of ambient brown carbon aerosol during wintertime heating season. However, understanding of relative contribution of different OA source factors to aerosol light scattering coefficient in $PM_{2.5}$ remain limited, especially under polluted urban environments.

Nanjing is located in the west of the Yangtze River Delta region, one of the three major urban agglomerations in China. This region is also the area of frequent haze pollution in China, and is the key area of air pollution prevention and control by the Chinese government. In this study, a coupled online observation system with a PM_1 quadrupole ACSM, a $PM_{2.5}$ quadrupole ACSM, and a photoacoustic extinctiometer (PAX) at 870 nm was set to measure non-refractory aerosol chemical composition in PM_1 and $PM_{2.5}$ and aerosol light scattering coefficient during haze and foggy episodes in Nanjing. In this work, the OA sources in different particle-size ranges (i.e., PM_1 and $PM_{2.5}$) were identified. The contribution of chemical composition (including organic composition) in $PM_{2.5}$ to aerosol scattering was quantified. The formation and evolution of SOA in PM_1 and $PM_{2.5}$ during typical foggy days were further analyzed. Finally, the influence of meteorological conditions on different aerosol components was investigated.

2. Methods and data analysis

The sampling site of this study was set up in the urban area of Nanjing, which can represent the typical megacity environment in the Yangtze River Delta region of China. The field observation experiment was carried out from 9 October to November 19, 2015, with the main purpose of capturing haze and foggy episodes. At the sampling site, we deployed the PM_1 and $PM_{2.5}$ quadrupole ACSMs, which were used to measure the chemical composition of NR-PM_1 and NR-$PM_{2.5}$ (including spectral data of organic matter), coupled with a PAX observation system to document the light scattering and absorption coefficients of $PM_{2.5}$. The standard calibration with ammonium nitrate particles at 300 nm was performed to determine the response factor of the two instruments, which were 1.09×10^{-10} (PM_1-ACSM) and 2.06×10^{-11} ($PM_{2.5}$-ACSM), respectively. The relative ionization efficiencies of ammonium (4.9 and 4.7) and sulfate (0.8 and 1.2) for the PM_1-ACSM and $PM_{2.5}$-ACSM were obtained from ammonium nitrate and ammonium sulfate particles, respectively. The default RIE values were used for nitrate (1.1), organics (1.4), and chloride (1.3), respectively (Canagaratna et al., 2007; Ng et al., 2011b). The composition-dependent collection efficiency was used for the mass concentration correction of the PM_1-ACSM species, while a CE of 1 was used for the $PM_{2.5}$-ACSM(Xu et al., 2017a). PM_1 and $PM_{2.5}$ aerodynamic focusing lens were used in PM_1-ACSM and $PM_{2.5}$-ACSM, respectively. The transmission efficiency of the two types of aerodynamic focusing lens can be found in previous studies (Liu et al., 2007; Williams et al., 2013b), respectively. More detailed description of the monitoring site can be found in our previous study (Zhang et al., 2017).

Quadrupole ACSM is of low resolution compared to high-resolution aerodyne Aerosol Mass Spectrometer (HR-ToF-AMS) (Canagaratna et al., 2007; DeCarlo et al., 2006). In practice, it was difficult for quadrupole ACSM to distinguish OA source factors with similar mass spectra, such as cooking and vehicle emission sources, based on traditional PMF method (Sun et al., 2012; Zhang et al., 2015c). To overcome this potential challenge, the PMF model equipped with ME2 algorithm

(Paatero, 1999) was used in this study for source apportionment of OA in NR-PM_1 and NR-$PM_{2.5}$. The ME2 algorithm can provide functionalities to constrain the model runs according to given reference data (e.g., factor profiles) from well-known sources (Canonaco et al., 2013). In this study, three primary organic factors, including HOA, COA and BBOA, was constrained, but OOA factor was unconstrained. The corresponding reference mass spectra were from our previous studies, including HOA and COA (Zhang et al., 2015b) and BBOA (Zhang et al., 2015c). In the ME2 runs, there is an important parameter, namely the constraint factor "**a**" value, which represents the freedom degree of the constraint. The larger the value is, the smaller the constraint force is, otherwise, the larger the constraint force is. In the specific calculation, the value of "**a**", we set varies from 0 to 0.4, and the average value of all the calculation results after obtaining the factor was as the final results. Finally, four factors were resolved, including three POA factors (HOA, COA and BBOA) and a SOA factor (i.e., OOA). Figure S1 presents good correlations for the results obtained between ME2 (constrained HOA, COA, and BBOA) and PMF (unconstrained mode), supporting acceptable outputs of the ME2 analysis. All ME2 analyses were performed based on the IGOR software package (SoFi) (Canonaco et al., 2013).

The PM_1 and $PM_{2.5}$ aerosol liquid water content (ALWC) – using PM_1-ACSM and $PM_{2.5}$-ACSM data – was calculated by ISORROPIA-II model (Fountoukis and Nenes, 2007). More detailed description for the calculation can be found in Zhang et al. (2017).

Random forest (RF) algorithm is an ensemble learning method for classification and regression tasks by taking decision tree as the basic unit and integrating multiple decision trees into an ensemble model. In essence, it combines several basic estimation units with weak performance into an ensemble model with strong performance. The "boost-strap" method is used to extract random samples from the training set for each decision tree, and the results are calculated separately. The final results are obtained after comprehensive consideration of each decision tree. RF can quantify the influence degree of each explanatory variable to the explained variable through importance so that the nonlinear influence of each explanatory variable can be directly reflected. In addition, the sensitivity analysis of the model and standardization of the results can specifically quantify the contribution rate of explanatory variables to the explained variables. RF has gradually been widely used in the field of atmospheric environment due to its strong learning ability and interpretability. Thanks to the above-mentioned properties that RF enjoys, the RF model was used in this work to explore the two following issues.

First, the contribution of the various $PM_{2.5}$ chemical components to the scattering coefficient of particulate matter was quantitatively analyzed. These substances include ammonium sulfate, ammonium nitrate, ammonium chloride and organic source factors. Among them, the mass concentration of ammonium salts ($(NH_4)_2SO_4$, NH_4NO_3, and NH_4Cl) was calculated according to the ion charge balance under the assumption that ammonium is sufficient (Wang et al., 2015, 2016). As shown in Eq. (1), the relative contribution (α) of each chemical composition and OA components to aerosol scattering coefficient was obtained through sensitivity analysis and standardization. This calculation methodology is comparable to a use in climate model to quantify contribution of each aerosol fractions to global radiative forcing (Li et al., 2016). The specific method was as follows, taking OOA as an example: OOA concentration obtained for each data point is decreased by 20% ($-\varepsilon_{OOA}$), and the predicted value was obtained after model prediction. The difference between the actual value (*all*) and the predicted value was used to obtain the change value of atmospheric scattering coefficient. Then, the concentration of all other chemical components was reduced by 20% ($-$ *RoPM*). Finally, the relative contribution of OOA to atmospheric scattering coefficient was obtained through normalization of OOA contribution.

The second issue investigated here using RF deals with the impact of meteorological conditions on aerosol chemical composition in the fine aerosol fractions. To do so, meteorological data included boundary layer height (BLH), solar radiation (SR), relative humidity (RH), air temperature (T2m), total precipitation (TP), wind speed (WS) and direction (WD), and total cloud cover (TCC). Among them, the BLH, SR, T2m, TP, and TCC were derived from the ERA5 reanalysis data of European Centre for Medium-Range Weather Forecasts (ECMWF), and other data were derived from ground meteorological stations. In order to make the results more stable, the importance of each explanatory variable was calculated by using the cross test of ten folds. All calculations were based on R language "Randomforest" package.

$$\alpha = \frac{[RF(all) - RF(-\varepsilon_{OOA})]}{2 \times RF(all) - RF(-\varepsilon_{OOA}) - RF(-RoPM)} \quad (1)$$

3. Results and discussion

3.1. Time-dependent and size-segregated chemical composition

Fig. 1 shows the time series of meteorological parameters, scattering and absorption coefficients and chemical composition (including inorganic and OA components) of atmospheric non-refractory fine particles during the whole observation period. In general, the NR-$PM_{2.5}$ mass concentration showed dynamic variations throughout the whole observation period. According to meteorological conditions and in agreement with our previous work (Zhang et al., 2017), we divided the whole observation period into five typical haze pollution and/or foggy episodes (i.e., Ep. 1- Ep. 5). In these different episodes, the concentrations and relative contributions of aerosol chemical components in different particle size ranges showed obvious differences (Zhang et al., 2017). For example, OA was mainly distributed in large-sized particles (i.e., NR-$PM_{1\text{-}2.5}$) during Ep. 2, with the contributions of NR-PM_1 OA and NR-$PM_{1\text{-}2.5}$ OA to the total NR-$PM_{2.5}$, being of 9% and 20%, respectively. During Ep. 4, OA was distributed equally between small-sized particles and larger-sized particles, with a 15% contribution to both NR-PM_1 OA and NR-$PM_{1\text{-}2.5}$ OA. These results illustrate that $PM_{2.5}$ mass size distributions vary from a pollution episode to another, also highlighting that monitoring the fine aerosol chemical composition in PM_1 only doesn't allow to reflect the actual picture of haze particles in China.

Fig. 2a shows the relative contribution of chemical composition of NR-PM_1 and NR-$PM_{1\text{-}2.5}$, respectively. Overall, the average mass concentration of NR-PM_1 was 53.2 μg m^{-3} during polluted days, which was about 5 times higher than that (11.6 μg m^{-3}) during clean days. The average mass concentration of NR-$PM_{2.5}$ was 99.2 μg m^{-3} during polluted days, which was about 4 times higher than that (23.9 μg m^{-3}) during clean days. The $PM_{1\text{-}2.5}$ accounted for a large fraction of the total NR-$PM_{2.5}$ during clean days (51%), which is comparable to the contribution (49%) during polluted days. This suggests roughly equivalent contributions of NR-PM_1 and NR-$PM_{1\text{-}2.5}$ to the total NR-$PM_{2.5}$ during clean and polluted periods. The contributions of NR-PM_1 and NR-$PM_{1\text{-}2.5}$ OAs to the total NR-$PM_{2.5}$ was of 21% (5.1 μg m^{-3}) and 22% (5.2 μg m^{-3}) during clean days, respectively. During polluted days, the contribution of PM_1 and $PM_{1\text{-}2.5}$ OAs to the total NR-$PM_{2.5}$ was of 19% (18.7 μg m^{-3}) and 14% (13.8 μg m^{-3}), respectively. The OA contributed the largest fraction, among all NR-$PM_{2.5}$ chemical composition, to the total NR-$PM_{2.5}$ during both clean (43%) and polluted (33%) days, respectively. These contributions were compared to the results regarding the contribution to NR-PM_1 observed by many previous studies in urban environment in eastern China (Zhou et al., 2020). The mass concentrations of NR-$PM_{1\text{-}2.5}$ OA during clean and polluted days were 6.6 μg m^{-3} and 19.4 μg m^{-3}, which were associated with the high contribution of 58% and 55% to the total NR-$PM_{2.5}$ OA mass, respectively. Possible origins of the OA sub-fractions are discussed in the following sub-section.

3.2. Size-dependent OA source apportionment outputs

Fig. 3 shows mass spectra and diel cycles of the OA source factors in

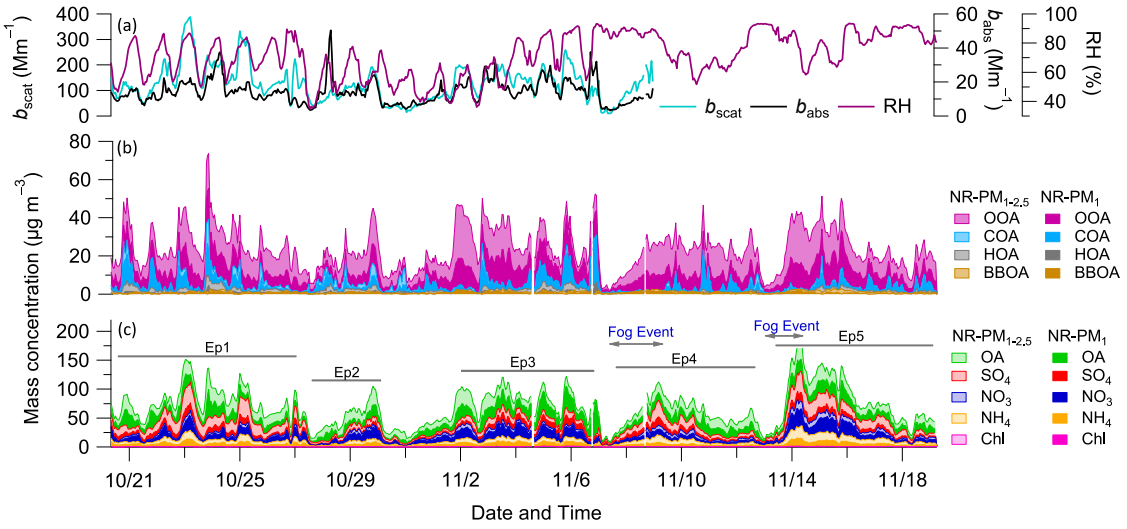

Fig. 1. Time series of meteorological factors, including (a) relative humidity, aerosol light scattering and absorption coefficients, and (b) PMF model calculated OA factors and (c) directly observed chemical composition in NR-PM$_1$ and NR-PM$_{2.5}$, respectively. Five pollution episodes (Ep 1–5), including two typical polluted fog events, were classified depending to the temporal variations.

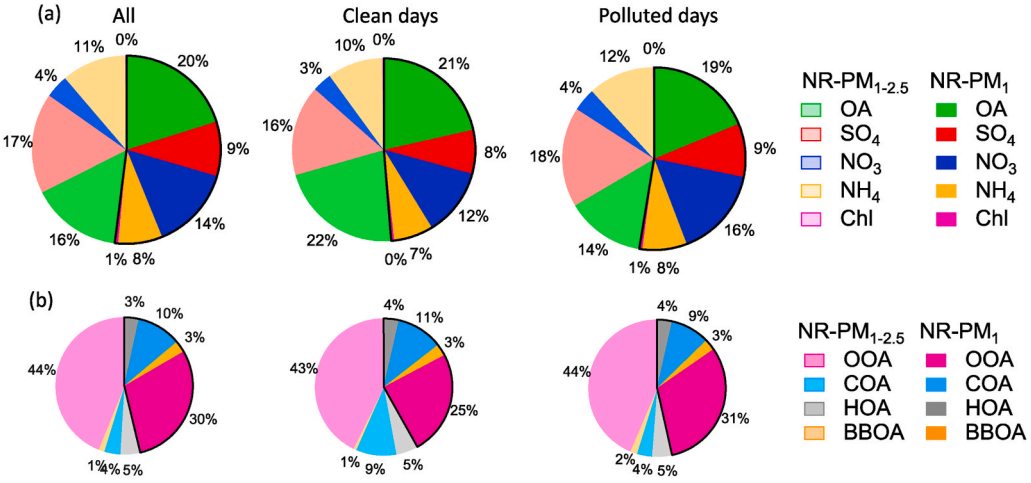

Fig. 2. Relative contribution of (a) chemical composition and (b) OA sources of PM$_1$ and PM$_{2.5}$ during relative clean and polluted air.

NR-PM$_1$ and NR-PM$_{2.5}$, including four source factors - i.e., HOA, COA, BBOA, and OOA - which are described hereafter. The mass concentration of COA presented high peaks at noon hours and 18:00–20:00, which is associated with intensive emissions of cooking around the sampling site area. After reaching the peak value, the concentration of COA decreased rapidly to about 1.5 μg m^{-3} and remained stable with such low concentrations, suggesting the fast removing of the COA particles from the atmosphere and showing the short lifetime characterization. On average, the COA was mainly present in NR-PM$_1$ (rather than in NR-PM$_{1\text{-}2.5}$, see Fig. 2b). However, enhanced mass concentration of COA could be observed in NR-PM$_{1\text{-}2.5}$ concomitantly with intensive cooking periods, which could indicate that COA in large-sized particle could be generated from fresh cooking emission.

HOA has been widely identified in the urban atmosphere, primarily associated with vehicle exhaust emissions (Li et al., 2017b; Zhang et al., 2011; Zhou et al., 2020). The diel variation of HOA in NR-PM$_1$ and NR-PM$_{2.5}$ showed obvious consistency in the peak time of vehicle emissions in the morning and evening (Fig. 3b), further supporting the link between these HOA factors with vehicle emissions. Interestingly, the signal intensity of *m/z* 44 ion fragments of HOA in NR-PM$_{2.5}$ was substantially higher than that of NR-PM$_1$. This may suggest that freshly emitted HOA particles were mainly distributed in the particle size range of PM$_1$, while HOA may undergo a rapid oxidation process after being emitted into the atmosphere and thus forming relatively aged HOA particles. Such large-sized HOA particles may contain some oxygen-containing components. In laboratory experiments, Robinson et al. (2007) found that particulate hydrocarbon organics emitted from combustion sources could undergo oxidation process and transform into SOA. In field observation, evidences that ambient HOA particles get oxidized rapidly through atmospheric processes have also been proposed recently (Cao et al., 2018). Based on these previous studies and the results of the present one, it could be then inferred that HOA particles in NR-PM$_{2.5}$ was likely more oxidized, which need to be verified by further field observations and laboratory combustion simulation experiments.

The BBOA mass concentrations were globally low, with average values of about 1 μg m^{-3} in both NR-PM$_1$ and NR-PM$_{2.5}$ size fractions. In addition, their contributions to the total OA were overall less than 5%, indicating that the sampling site might be benefiting negligible impact of biomass burning plumes transported from the surrounding areas of Nanjing during the observation period. Finally, the mass spectra of both NR-PM$_{2.5}$ OOA and NR-PM$_1$ OOA were characterized by high

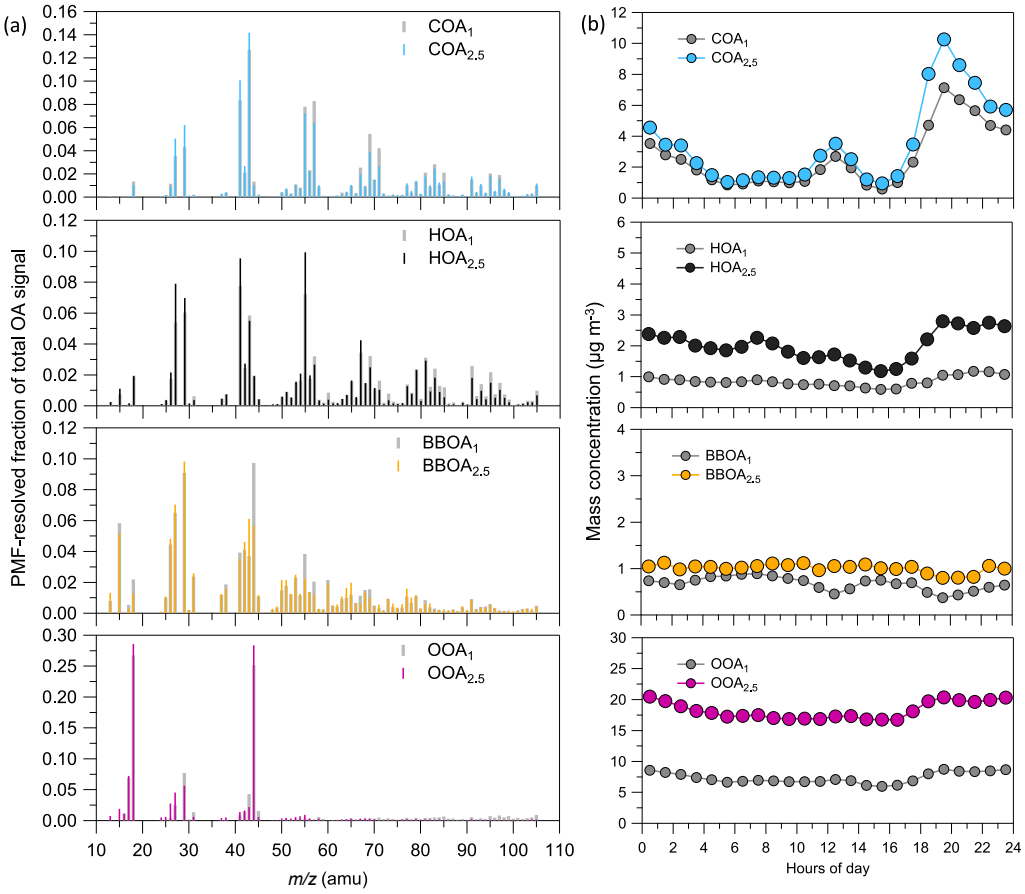

Fig. 3. Mass spectra and diurnal variations of NR-PM_1 and NR-$PM_{2.5}$ OA factors.

contribution of *m/z* 44 (CO_2^+), which is consistent with previous results (Zhang et al., 2007, 2011). The NR-PM_1 and NR-$PM_{2.5}$ OOAs showed very similar diel patterns (Fig. 3b), and their concentrations gradually increased during nighttime. There were two possible reasons for the high OOA concentrations during nighttime. One was the low boundary layer height and weak horizontal wind speed during nighttime, which could lead to weak atmospheric dilution and then accumulation of air pollution (An et al., 2019; Ding et al., 2016). Another reason was that nocturnal chemistry might promote the formation of SOA (Huang et al., 2020; Li et al., 2017a; Wang et al., 2021; Zhou et al., 2020). The effect of nighttime aqueous processes on the observed OOAs will be further discussed in the following section 3.4.

Moreover, the NR-$PM_{1\text{-}2.5}$ OOA accounted for 43% (4.8 μg m^{-3}) and 44% (15.8 μg m^{-3}) of the total NR-$PM_{2.5}$ OA mass, respectively (see Fig. 2b). The NR-$PM_{1\text{-}2.5}$ OOA increased by 18% and 13% during clean and polluted days, respectively, as a comparison of the NR-PM_1 OOA. These results suggest substantial contribution of large-sized OA particles, especially the SOA factor, to fine particles during both clean and polluted days. The contributions of the NR-$PM_{1\text{-}2.5}$ COA to the total OA during clean and polluted days were 9% and 4%, which showed an obvious increase during clean days compared to polluted days. The contribution of NR-PM_1 OOA to the total OA mass during polluted days was 31%, which was higher than that during clean days (25%). During the two foggy episodes, the OOA made major contribution to the total OA mass. For example, the OOA accounted for 86% and 83% of the total OA mass during the two foggy episodes, along with high contributions by the NR-$PM_{2.5}$ OOA (56% and 52%), respectively. These results highlighted high contribution of OOA to the NR-$PM_{2.5}$, especially during foggy episodes under high relative humidity conditions.

3.3. Influences of the chemical components on aerosol scattering coefficient

As shown in Fig. 1, the light scattering coefficient of $PM_{2.5}$ keeps an overall consistent trend with the relative humidity of ambient air, reflecting potential link between relative humidity and the formation of light-scattering aerosol chemical composition. Fig. 4 shows the relative contributions of different NR-$PM_{2.5}$ chemical components and OA source factors to the total $PM_{2.5}$ scattering coefficient during haze and foggy episodes. On average, the ammonium sulfate (37%) contributed a largest fraction to the total $PM_{2.5}$ scattering coefficient, followed by OOA (25%) and ammonium nitrate (24%), yet with low contribution from POA factors, e.g., COA (1%).

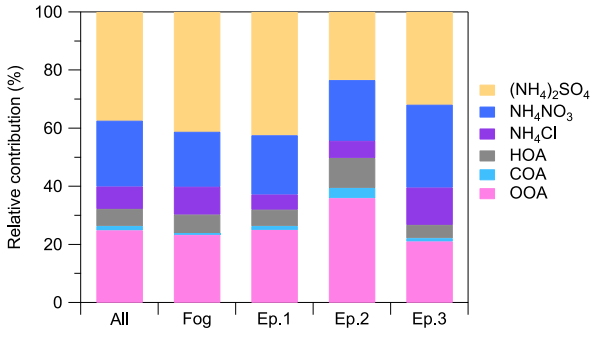

Fig. 4. Relative contribution of NR-$PM_{2.5}$ chemical composition and OA factors to aerosol light scattering coefficient during the entire periods (All), foggy days (Fog), and three typical haze episodes (i.e., Ep. 1, Ep. 2, and Ep. 3).

3.4. Evolution and formation of OOA during foggy episodes

Fig. 5 shows the relationship of the OOA to CO ratio in both NR-PM_1 and NR-$PM_{2.5}$ (OOA_1/CO and $OOA_{2.5}$/CO), as well as the OOA ratio between NR-$PM_{2.5}$ and NR-PM_1 ($OOA_{2.5}/OOA_1$), as a function of time during the two foggy episodes. The so called 'CO-ratio method' was often used to minimize the influence of atmospheric dilution on variation of air pollutants and then to capture the influence mainly due to chemical process and/or emissions [11, 52, 53](Ding et al., 2019; Hu et al., 2013; Zheng et al., 2018). Both OOA_1/CO and $OOA_{2.5}$/CO ratios during each foggy episode showed obviously increasing trend over time, indicating the formation of OOA during foggy episodes. Meanwhile, the $OOA_{2.5}/OOA_1$ ratio also presented an increasing trend over time, which could be characterized by an exponential function (see Fig. 5). This may reflect the formation of SOA in large-sized particles, i.e., NR-$PM_{1\text{-}2.5}$, probably via aqueous processes.

Fig. 6 presents the relationship between OOA and aerosol liquid water content (ALWC) during foggy episodes and nighttime. ALWC is commonly used as indicative of aqueous chemical process in field observation experiments (Huang et al., 2020; Sun et al., 2016; Xiao et al., 2021; Xu et al., 2017b). The mass concentrations of OOA_1 and $OOA_{2.5}$ increased with increase of ALWC during foggy episodes, which is similar to the patterns during nighttime. These results suggest that the formation of OOA factors might be associated with aqueous processes during foggy episodes and nighttime. As reported by previous studies, atmospheric aqueous chemical processes could make important contribution to OOA_1 during haze episodes in northeastern China (Huang et al., 2019; Li et al., 2017a; Sun et al., 2016; Wang et al., 2021). To further support the important impact of ALWC on the OOA formation, random forest modeling was used to examine the importance of different variables to the concentration variations of OOA_1 and $OOA_{2.5}$ (see Fig. 7). As shown in Fig. 7, ALWC was of the main responsible for the changes in OOA_1 and $OOA_{2.5}$ concentrations, supporting that aqueous phase chemistry might contribute the OOA formation during foggy episodes and nighttime. In addition, the ratio between OOA_1 and $OOA_{2.5}$ was enhanced at the conditions of high ALWC concentrations, further suggesting the large-sized OOA formation involved in atmospheric aqueous process.

3.5. Potential impact of meteorological conditions on OA factors

Fig. 8 exhibits the mass concentrations of OA factors as functions of WS and BLH, respectively. Except for BBOA, the mass concentrations of OA factors in both NR-PM_1 and NR-$PM_{2.5}$ decreased with the increase of WS or BLH, indicating that atmospheric dilution had influence on the variation of these OA factors. Indeed, COA decreased significantly with the increase of WS and BLH, indicating that the concentration levels of COA was significantly affected by atmospheric dilution. Negligible change in mass concentration of the two BBOA factors as the function of

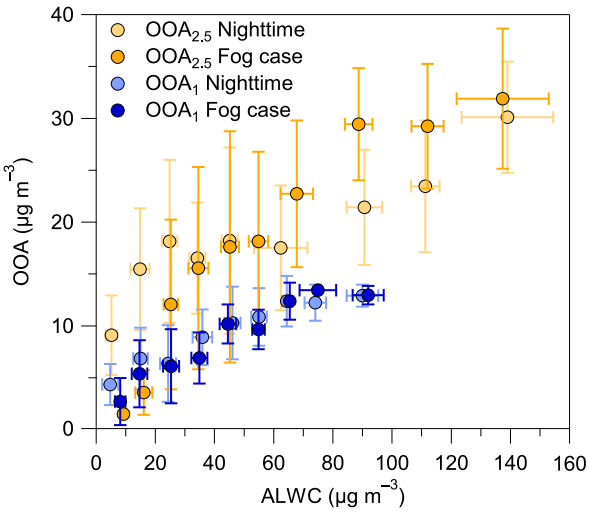

Fig. 6. Relationship between OOA factors and ALWC during foggy days and during nighttime across the entire observation period.

WS and BLH was found, which might reflect a background concentration of BBOA factor in both PM_1 and $PM_{2.5}$ during the observation period. Compared with HOA and COA, the decreasing trend of OOA as increase of WS and BLH was relatively small, likely reflecting the regional pollution characteristics of such SOA factor.

To further investigate impact of meteorological conditions on variations of OOA factors, random forest modeling was applied to test the importance of meteorological factors. Figure S2 shows the importance distribution of various meteorological condition factors obtained from the random forest modeling. As indicated by the results of Fig. S2, BLH and WS have important effects on each NR-$PM_{2.5}$ species, which could further support important of role of atmospheric dilution in affecting variations of both primary and secondary NR-$PM_{2.5}$ OA factors during polluted episodes. BLH was the main importance factor for HOA and COA factors, indicates that the change of boundary layer has an important influence on the concentration variation of HOA and COA. In addition, WS was an important meteorological parameter influencing the BBOA variations, which could be partly explained by horizontal transport of biomass burning emissions around Nanjing (Zhang et al., 2015c). In addition to BLH and WS, relative humidity and total cloud coverage had an important influence on both OOA_1 and $OOA_{2.5}$ factors, again suggesting that aqueous processes have a potential contribution to the formation of OOA during the observation period.

4. Conclusion

The sources, processes, and optical properties of organics in NR-PM_1

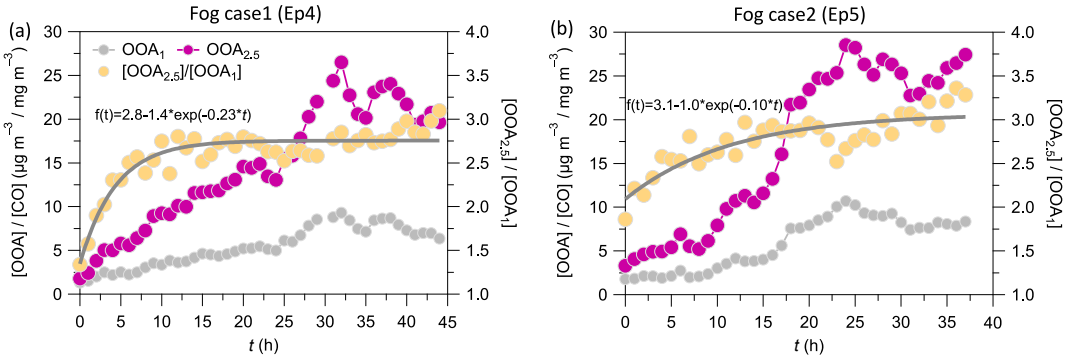

Fig. 5. Evolution of the ratio of OOA to CO in NR-$PM_{2.5}$ or NR-PM_1 and the ratio of $[OOA_{2.5}]/[OOA_1]$ during the two foggy-days' periods, i.e., (a) Ep. 4 and (b) Ep. 5, respectively.

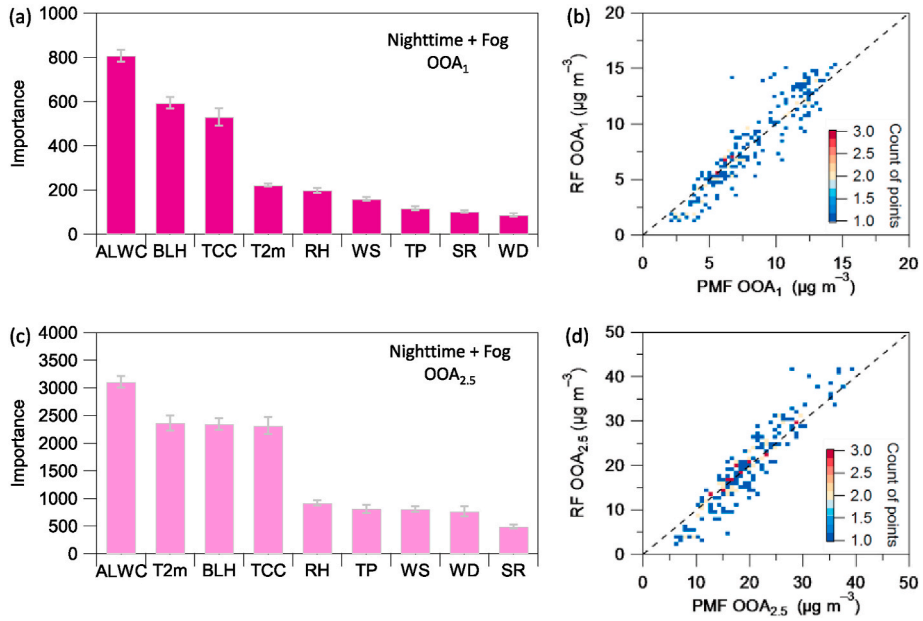

Fig. 7. Variable importance (a and c), where variables include boundary layer height (BLH), solar radiation (SR), relative humidity (RH), air temperature (T2m), total precipitation (TP), wind speed (WS) and direction (WD), and total cloud cover (TCC), and correlation (b and d) between RF predicted and PMF calculated (a and b) OOA_1 and (c and d) $OOA_{2.5}$ during nighttime, respectively. The "count of points" in (b) and (d) indicates the number of data points for each dot.

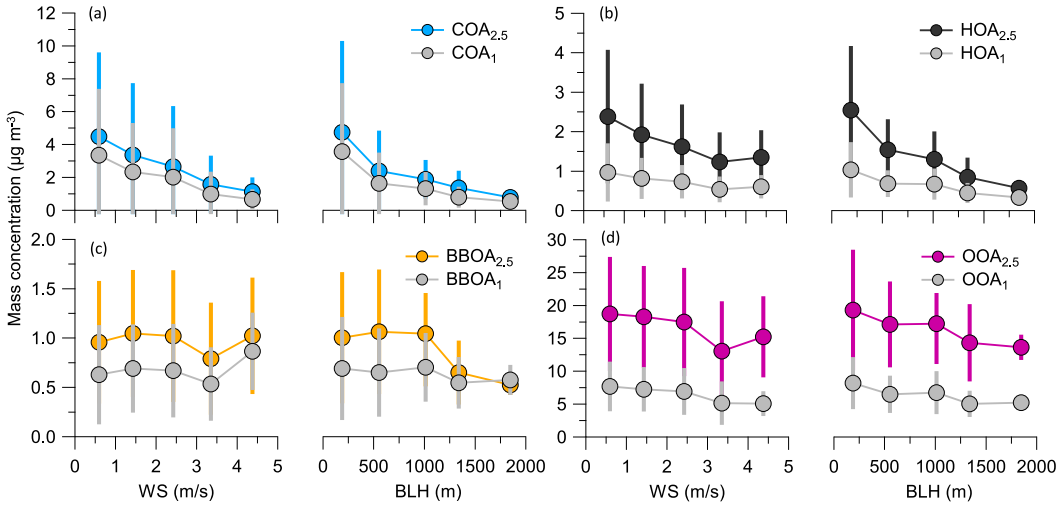

Fig. 8. Comparison of NR-PM_1 and NR-$PM_{2.5}$ OA factors as a function of wind speed (WS) and boundary layer height (BLH), respectively.

and NR-$PM_{2.5}$ during haze and foggy episodes in urban Nanjing have been investigated based on synchronous online measurements of two ACSMs (for NR-PM_1 and NR-$PM_{2.5}$) and a PAX as well as subsequent comprehensive statistical analysis. Four-factor solution (i.e., COA, HOA, BBOA, and OOA) for both NR-PM_1 and NR-$PM_{2.5}$ OAs was achieved using PMF analysis of ACSM organic mass spectral data. Overall, the contributions of these factors to NR-PM_1 and NR-$PM_{2.5}$ OAs were 21% and 16% (COA), 7% and 9% (HOA), 5% and 5% (BBOA), and 58% and 82% (OOA), respectively. During haze episodes, OOA in NR-$PM_{1\text{-}2.5}$ showed a high contribution (49%) to total NR-$PM_{2.5}$ OA, indicating that SOA formation in large-sized particles has an important contribution to haze particles. Meanwhile, substantially enhanced formation of OOA factors as a function of time during foggy episodes was observed, where the ratio of $OOA_{2.5}$ to OOA_1 presented an exponent function as time. These OOA factors increased clearly as increased of ALWC, which is comparable to the largest important impact of ALWC on OOA variations tested by random forest model. These results indicated that the formation of such OOA factors might be involved in aqueous chemistry during foggy days, especially with high contribution to large-sized SOA particles. Evident increase in the NR-$PM_{1\text{-}2.5}$ COA by mass was observed at intensive cooking emission hours, indicating that the urban cooking source sector may contribute to large-sized COA particles. The NR-$PM_{2.5}$ HOA presented higher oxidation level and mass concentration than these of HOA in NR-PM_1, which might indicate that large-sized HOA particles were associated with more oxidized POA particles. Based on random forest modeling, the contribution of NR-$PM_{2.5}$ chemical composition to aerosol light scattering coefficient was quantified as follows: $(NH_4)_2SO_4$ (23%), NH_4NO_3 (21%), NH_4Cl (6%), HOA (1%), COA (4%), and OOA (35%), respectively. These results indicate that secondary inorganic and organic aerosols play an important role in solar radiation scattering and influencing atmospheric visibility during haze and/or foggy episodes. According to current emission scenarios and their feedbacks to air quality, controlling anthropogenic SOA precursors (i.e., volatile organic compounds, VOCs), play an important role in air

quality and climate change mitigation. Analysis of impact of meteorological parameters on the OA factors suggested that atmospheric dilution significantly affect concentration levels of OA factors, especially for POA particles, such as HOA and COA.

Author contributions

Shuaiyi Li: Formal analysis, Software, Writing – original draft; **Cheng Chen**: Data curation, Writing – review & editing; and **Lili Tang**: Data curation, Writing – review & editing; **Guang-li Yang**: Writing – review & editing; **Jie Fang**: Writing – review & editing; **Yele Sun**: Writing – review & editing; **Hongli Wang**: Writing – review & editing; **Hongliang Zhang**: Data curation. **Philip L. Croteau**: Data curation, Writing – review & editing; and **John T. Jayne**: Data curation, Writing – review & editing; **Hong Liao**: Funding acquisition, Writing – review & editing. and **Xinlei Ge**: Funding acquisition, Writing – review & editing. **Olivier Favez**: Methodology, Software, Writing – review & editing; **Yunjiang Zhang**: Funding acquisition, Conceptualization, Data curation, Formal analysis, Investigation, Methodology, Validation, Software, Supervision, Writing – original draft, Writing – review & editing.

Declaration of competing interest

The authors declare that they have no known competing financial interests or personal relationships that could have appeared to influence the work reported in this paper.

Acknowledgements

This study was supported by Natural Science Foundation of Jiangsu Province (grant no. BK20210663), State Environmental Protection Key Laboratory of Formation and Prevention of Urban Air Pollution Complex (grant no. CX2020080579), and the Natural Science Foundation of China (grant no. 21976093 and grant no. 42021004).

Appendix A. Supplementary data

Supplementary data to this article can be found online at https://doi.org/10.1016/j.envres.2022.113557.

References

An, Z., et al., 2019. Severe haze in northern China: a synergy of anthropogenic emissions and atmospheric processes. Proc. Natl. Acad. Sci. U. S. A. 116, 8657–8666.
Canagaratna, M.R., et al., 2007. Chemical and microphysical characterization of ambient aerosols with the aerodyne aerosol mass spectrometer. Mass Spectrom. Rev. 26, 185–222.
Canonaco, F., et al., 2013. SoFi, an IGOR-based interface for the efficient use of the generalized multilinear engine (ME-2) for the source apportionment: ME-2 application to aerosol mass spectrometer data. Atmos. Meas. Tech. 6, 3649–3661.
Cao, J.-j., et al., 2012. Impacts of aerosol compositions on visibility impairment in Xi'an, China. Atmos. Environ. 59, 559–566.
Cao, L.-M., et al., 2018. Volatility measurement of atmospheric submicron aerosols in an urban atmosphere in southern China. Atmos. Chem. Phys. 18, 1729–1743.
DeCarlo, P.F., et al., 2006. Field-deployable, high-resolution, time-of-flight aerosol mass spectrometer. Anal. Chem. 78, 8281–8289.
Ding, A., et al., 2019. Significant reduction of PM2.5 in eastern China due to regional-scale emission control: evidence from SORPES in 2011–2018. Atmos. Chem. Phys. 19, 11791–11801.
Ding, A.J., et al., 2016. Enhanced haze pollution by black carbon in megacities in China. Geophys. Res. Lett. 43, 2873–2879.
He, K., et al., 2001. The characteristics of PM2.5 in Beijing, China. Atmos. Environ. 35, 4959–4970.
Hu, M., et al., 2015. Insight into characteristics and sources of PM2.5 in the Beijing-Tianjin-Hebei region, China. Natl. Sci. Rev. 2, 257–258.
Hu, W., et al., 2017. Evaluation of the new capture vaporizer for aerosol mass spectrometers (AMS) through field studies of inorganic species. Aerosol Sci. Technol. 51, 735–754.
Hu, W.W., et al., 2013. Insights on organic aerosol aging and the influence of coal combustion at a regional receptor site of central eastern China. Atmos. Chem. Phys. 13, 10095–10112.
Huang, R.-J., et al., 2020. Contrasting sources and processes of particulate species in haze days with low and high relative humidity in wintertime Beijing. Atmos. Chem. Phys. 20, 9101–9114.
Huang, R.-J., et al., 2019. Primary emissions versus secondary formation of fine particulate matter in the most polluted city (Shijiazhuang) in North China. Atmos. Chem. Phys. 19, 2283–2298.
Huang, X.F., et al., 2012. Highly time-resolved chemical characterization of atmospheric fine particles during 2010 Shanghai World Expo. Atmos. Chem. Phys. 12, 4897–4907.
IPCC, 2013. Climate Change 2013: the Physical Science Basis. Contribution of Working Group I to the Fifth Assessment Report of the Intergovernmental Panel on Climate Change.
Joo, T., et al., 2021. Evaluation of a new aerosol chemical speciation monitor (ACSM) system at an urban site in atlanta, ga: the use of capture vaporizer and PM2.5 inlet. ACS Earth Space Chem 5, 2565–2576.
Li, B., et al., 2016. The contribution of China's emissions to global climate forcing. Nature 531, 357–361.
Li, H., et al., 2017a. Wintertime aerosol chemistry and haze evolution in an extremely polluted city of the North China Plain: significant contribution from coal and biomass combustion. Atmos. Chem. Phys. 17, 4751–4768.
Li, H., et al., 2018. Nitrate-driven urban haze pollution during summertime over the North China Plain. Atmos. Chem. Phys. 18, 5293–5306.
Li, Y.J., et al., 2017b. Real-time chemical characterization of atmospheric particulate matter in China: a review. Atmos. Environ. 158, 270–304.
Lin, C., et al., 2018. Extreme air pollution from residential solid fuel burning. Nat. Sustain. 1, 512–517.
Liu, P.S.K., et al., 2007. Transmission efficiency of an aerodynamic focusing lens system: comparison of model calculations and laboratory measurements for the aerodyne aerosol mass spectrometer. Aerosol. Sci. Technol. 41, 721–733.
Ng, N.L., et al., 2011a. Real-time methods for estimating organic component mass concentrations from aerosol mass spectrometer data. Environ. Sci. Technol. 45, 910–916.
Ng, N.L., et al., 2011b. An aerosol chemical speciation monitor (ACSM) for routine monitoring of the composition and mass concentrations of ambient aerosol. Aerosol Sci. Technol. 45, 780–794.
Paatero, P., 1999. The multilinear engine—a table-driven, least squares program for solving multilinear problems, including the n-way parallel factor Analysis model. J. Comput. Graph Stat. 8, 854–888.
Robinson, A.L., et al., 2007. Rethinking organic aerosols: semivolatile emissions and photochemical aging. Science 315, 1259–1262.
Sun, Y., et al., 2016. Primary and secondary aerosols in Beijing in winter: sources, variations and processes. Atmos. Chem. Phys. 16, 8309–8329.
Sun, Y., et al., 2020. Chemical differences between PM 1 and PM 2.5 in highly polluted environment and implications in air pollution studies. Geophys. Res. Lett. 47.
Sun, Y., et al., 2012. Characterization of summer organic and inorganic aerosols in beijing, China with an aerosol chemical speciation monitor. Atmos. Environ. 51, 250–259.
Sun, Y., et al., 2018. Source apportionment of organic aerosol from 2-year highly time-resolved measurements by an aerosol chemical speciation monitor in Beijing, China. Atmos. Chem. Phys. 18, 8469–8489.
Sun, Y.L., et al., 2015. Long-term real-time measurements of aerosol particle composition in Beijing, China: seasonal variations, meteorological effects, and source analysis. Atmos. Chem. Phys. 15, 10149–10165.
Sun, Y.L., et al., 2013. Aerosol composition, sources and processes during wintertime in Beijing, China. Atmos. Chem. Phys. 13, 4577–4592.
Wang, J., et al., 2016. Highly time-resolved urban aerosol characteristics during springtime in Yangtze River Delta, China: insights from soot particle aerosol mass spectrometry. Atmos. Chem. Phys. 16, 9109–9127.
Wang, J., et al., 2021. Aqueous production of secondary organic aerosol from fossil-fuel emissions in winter Beijing haze. Proc. Natl. Acad. Sci. U. S. A. 118.
Wang, Q., et al., 2015. Chemical composition of aerosol particles and light extinction apportionment before and during the heating season in Beijing, China. J. Geophys. Res. Atmos. 120, 12708–12722.
Williams, L.R., et al., 2013a. Characterization of an aerodynamic lens for transmitting particles greater than 1 micrometer in diameter into the Aerodyne aerosol mass spectrometer. Atmos. Meas. Tech. 6, 3271–3280.
Williams, L.R., et al., 2013b. Characterization of an aerodynamic lens for transmitting particles greater than 1 micrometer in diameter into the Aerodyne aerosol mass spectrometer. Atmos. Meas. Tech. 6, 3271–3280.
Xiao, Y., et al., 2021. Insights into aqueous-phase and photochemical formation of secondary organic aerosol in the winter of Beijing. Atmos. Environ. 259.
Xie, C., et al., 2019. Vertical characterization of aerosol optical properties and brown carbon in winter in urban Beijing, China. Atmos. Chem. Phys. 19, 165–179.
Xu, W., et al., 2016. Laboratory characterization of an aerosol chemical speciation monitor with PM2.5 measurement capability. Aerosol Sci. Technol. 51, 69–83.
Xu, W., et al., 2017a. Laboratory characterization of an aerosol chemical speciation monitor with PM2.5 measurement capability. Aerosol Sci. Technol. 51, 69–83.
Xu, W., et al., 2017b. Effects of aqueous-phase and photochemical processing on secondary organic aerosol formation and evolution in beijing, China. Environ. Sci. Technol. 51, 762–770.
Xu, W., et al., 2020. Mass spectral characterization of primary emissions and implications in source apportionment of organic aerosol. Atmos. Meas. Tech. 13, 3205–3219.
Zhang, Q., et al., 2007. Ubiquity and dominance of oxygenated species in organic aerosols in anthropogenically-influenced Northern Hemisphere midlatitudes. Geophys. Res. Lett. 34 (n/a-n/a).

Zhang, Q., et al., 2011. Understanding atmospheric organic aerosols via factor analysis of aerosol mass spectrometry: a review. Anal. Bioanal. Chem. 401, 3045–3067.
Zhang, Q., et al., 2019a. Drivers of improved PM2.5 air quality in China from 2013 to 2017. Proc. Natl. Acad. Sci. U.S.A. 116, 24463–24469.
Zhang, R., et al., 2015a. Formation of urban fine particulate matter. Chem. Rev. 115, 3803–3855.
Zhang, Y., et al., 2020a. Substantial brown carbon emissions from wintertime residential wood burning over France. Sci. Total Environ. 743, 140752.
Zhang, Y., et al., 2018. Evidence of major secondary organic aerosol contribution to lensing effect black carbon absorption enhancement. npj Clim. Atmos. Sci. 1, 47.
Zhang, Y., et al., 2019b. Six-year source apportionment of submicron organic aerosols from near-continuous highly time-resolved measurements at SIRTA (Paris area, France). Atmos. Chem. Phys. 19, 14755–14776.
Zhang, Y., et al., 2017. Field characterization of the PM2.5 Aerosol Chemical Speciation Monitor: insights into the composition, sources, and processes of fine particles in eastern China. Atmos. Chem. Phys. 17, 14501–14517.
Zhang, Y., et al., 2015b. Chemical composition, sources and evolution processes of aerosol at an urban site in Yangtze River Delta, China during wintertime. Atmos. Environ. 123, 339–349.
Zhang, Y., et al., 2020b. Aerosol measurements by soot particle aerosol mass spectrometer: a review. Curr. Pollut. Rep. 6, 440–451.
Zhang, Y.J., et al., 2015c. Insights into characteristics, sources, and evolution of submicron aerosols during harvest seasons in the Yangtze River delta region, China. Atmos. Chem. Phys. 15, 1331–1349.
Zhang, Y.L., Cao, F., 2015. Fine particulate matter (PM 2.5) in China at a city level. Sci. Rep. 5, 14884.
Zhang, Y.M., et al., 2014. Chemical composition and mass size distribution of PM1 at an elevated site in central east China. Atmos. Chem. Phys. 14, 12237–12249.
Zheng, B., et al., 2018. Trends in China's anthropogenic emissions since 2010 as the consequence of clean air actions. Atmos. Chem. Phys. 18, 14095–14111.
Zhou, W., et al., 2020. A review of aerosol chemistry in Asia: insights from aerosol mass spectrometer measurements. Environ. Sci.: Process. Impacts 22, 1616–1653.